Pears, B., et al., 2020, A sub-centennial-scale optically stimulated luminescence chronostratigraphy and late Holocene flood history from a temperate river confluence: Geology, v. 48, https://doi.org/10.1130/G47079.1

Supplemental Material

Content

Supplemental Data Files

S1. Topographic & Historic Landscape Modelling

Topographic modelling at Powick Hams and the Severn-Teme confluence was conducted using high-resolution LiDAR datasets available from the UK Ordnance Survey and Environment Agency. Initially a Digital Terrain Model (DTM) at 50m resolution was created for the entire Severn catchment and overlain by major rivers (Figure 1A) (UK Ordnance Survey, 2016). A more detailed DTM at 1m resolution was then created for a 3.5km^2 area across the Severn-Teme confluence and overlain by a colour shaded elevation model and major watercourses (Figure 1B) (UK Environment Agency, 2016). Historic strip fields and enclosures illustrated on the Coventry Map (Coventry Map, 1648) and from the 1st Edition Ordnance Survey (UK Ordnance Survey, 1886) were exported into GIS and digitised as an additional layer (Figure 1B). Historic assets were determined from the Worcestershire Historic Environment Record (WHER, 2017).

In order to contextualise the sequence stratigraphy across the wider floodplain landscape, existing core data held by the British Geological Survey (https://www.bgs.ac.uk/data/bmd.html) (British Geological Survey, 2017) and academic work (Brown, 1983a+b; 1985; 1987) was gathered and remodelled with the new data in cross sections. The ground surface topography across each transect was extracted from the raw LiDAR data at 10cm resolution (Figure 1C).

S2. Field Sampling

In order to analyse the sedimentary sequence at Powick Hams a river section was excavated along the banks of the River Teme (Lat: 52.169259, Lon: -2.2376946). The sample section was cleaned, photographed and recorded and revealed 5.3m of alluvium down to the present river level, with terrace gravels identified at the base. From the section in-situ sediment samples were collected using u-channels to enable 1cm resolution analysis and 'dark' bulk samples collected every 5cm specifically for pOSL analysis (See Supplementary Material S10).

S3. Optically Stimulated Luminescence (OSL) Methodology and Data

From the section, 8 sealed Optically Stimulated Luminescence (OSL) (Huntley et al., 1985; Aitken, 1998) sediment samples were collected within opaque tubing and submitted for optical dating at the University of Gloucestershire (Toms and Wood, 2018), (Table 1, Figure 2).

Sample Preparation

To preclude optical erosion of the datable signal prior to measurement, all samples were opened and prepared under controlled laboratory illumination provided by Encapsulite RB-10 (red) filters. To isolate that material potentially exposed to daylight during sampling, sediment located within 20 mm of each tube-end was removed. The remaining sample was dried and then sieved. Depending upon each sample's modal grain size, quartz within the fine sand or fine silt fraction was segregated.

Samples were then segregated and subjected to acid and alkaline digestion (10% HCl, 15% H_2O_2) to attain removal of carbonate and organic components respectively. For fine sand fractions, a further acid digestion in HF (40%, 60 mins) was used to etch the outer 10-15 µm layer affected by α radiation and degrade each samples' feldspar content. During HF treatment, continuous magnetic stirring was used to effect isotropic etching of grains. 10% HCl was then added to remove acid soluble fluorides. Each sample was dried, resieved and quartz isolated from the remaining heavy mineral fraction using a sodium polytungstate density separation at 2.68g.cm^{-3}. Twelve 8 mm multi-grain aliquots (c. 3-6 mg) of quartz from each sample were then mounted on aluminium discs for determination of De values. Fine silt sized quartz, along with other mineral grains of varying density and size, was extracted by sample sedimentation in acetone (<15 µm in 2 min 20 s, >5 µm in 21 mins at 20ºC). Feldspars and amorphous silica were then removed from this fraction through acid digestion (35% H_2SiF_6 for 2 weeks, Jackson et al., 1976; Berger et al., 1980). Following addition of 10% HCl to

remove acid soluble fluorides, grains degraded to <5 μm as a result of acid treatment were removed by acetone sedimentation. Twelve multi-grain aliquots (ca. 1.5 mg) were then mounted on aluminium discs for D_e evaluation. All drying was conducted at 40°C to prevent thermal erosion of the signal.

D_e Measurements

The estimation of D_e acquired since burial requires calibration of the natural signal using known amounts of laboratory dose. D_e values were quantified using a single-aliquot regenerative-dose (SAR) protocol (Murray and Wintle 2000; 2003) facilitated by a Risø TL-DA-15 irradiation-stimulation-detection system (Markey et al., 1997; Bøtter-Jensen et al., 1999) and using the Analyst package (Duller, 2015). Within this apparatus, optical signal stimulation is provided by an assembly of blue diodes (5 packs of 6 Nichia NSPB500S), filtered to 470±80 nm conveying 15 $mW.cm^{-2}$ using a 3 mm Schott GG420 positioned in front of each diode pack. Infrared (IR) stimulation, provided by 6 IR diodes (Telefunken TSHA 6203) stimulating at 875±80nm delivering ~5 $mW.cm^{-2}$, was used to indicate the presence of contaminant feldspars (Hütt et al., 1988). Stimulated photon emissions from quartz aliquots are in the ultraviolet (UV) range and were filtered from stimulating photons by 7.5 mm HOYA U-340 glass and detected by an EMI 9235QA photomultiplier fitted with a blue-green sensitive bialkali photocathode. Aliquot irradiation was conducted using a 1.48 GBq $^{90}Sr/^{90}Y$ β source calibrated for multi-grain aliquots of 5-15 and 125-180 μm quartz against the 'Hotspot 800' ^{60}Co γ source located at the National Physical Laboratory (NPL), UK.

The propensity of feldspar signals to fade and underestimate age, coupled with their higher sensitivity relative to quartz makes it imperative to quantify feldspar contamination. At room temperature, feldspars generate a signal (Infrared Stimulated Luminescence; IRSL) upon exposure to IR whereas quartz does not. The signal from feldspars contributing to OSL can be depleted by prior exposure to IR. For all aliquots the contribution of any remaining feldspars was estimated from the OSL IR depletion ratio (Duller, 2003). The influence of IR depletion on the OSL signal can be illustrated by comparing the regenerated post-IR OSL D_e with the applied regenerative-dose. If the addition to OSL by feldspars is insignificant, then the repeat dose ratio of OSL to post-IR OSL should be statistically consistent with unity, as is the case in this study.

Preheating aliquots between irradiation and optical stimulation is necessary to ensure comparability between natural and laboratory-induced signals. However, the multiple irradiation and preheating steps that are required to define single-aliquot regenerative-dose response leads to signal sensitisation, rendering calibration of the natural signal inaccurate. The SAR protocol (Murray and Wintle, 2000; 2003) enables this sensitisation to be monitored and corrected using a test dose, here set at 5 Gy preheated to 220°C for 10s, to track signal sensitivity between irradiation-preheat steps. However, the accuracy of sensitisation correction for both natural and laboratory signals can be preheat dependent.

The Dose Recovery test was used to assess the optimal preheat temperature for accurate correction and calibration of the time dependent signal. Dose Recovery attempts to quantify the combined effects of thermal transfer and sensitisation on the natural signal, using a precise lab dose to simulate natural dose. The preheat chosen for each sample was that where the ratio between the applied dose and recovered D_e value was consistent with unity. Further thermal treatments, prescribed by Murray and Wintle (2000; 2003), were applied to optimise accuracy and precision. Optical stimulation occurred at 125°C in order to minimise effects associated with photo-transferred thermoluminescence and maximise signal to noise ratios. Inter-cycle optical stimulation was conducted at 280°C to minimise recuperation.

Murray and Wintle (2000; 2003) suggest recycling ratios from repeat dose measurements indicate the success of sensitivity correction, whereby ratios ranging across 0.9-1.1 are acceptable. However, this variation of repeat dose ratios in the high-dose region can have a significant impact on D_e interpolation. In this study, the recycling ratios are based on repeats of low and high dose measurements. All recycling ratios are consistent with the range 0.9-1.1, though the data is relatively scattered owing to poor signal to noise ratios.

D_r Measurements

Lithogenic D_r values were defined through measurement of U, Th and K radionuclide concentration and conversion of these quantities into α, β and γ D_r values (Table 1). α and β contributions were estimated from sub-samples by laboratory-based γ spectrometry using an Ortec GEM-S high purity Ge coaxial detector system, calibrated using certified reference materials supplied by CANMET. γ dose rates were estimated *in situ* using an EG&G μNomad portable NaI gamma spectrometer (calibrated using the block standards at RLAHA, University of Oxford); these reduce uncertainty relating to potential heterogeneity in the γ dose field surrounding each sample. The level of U disequilibrium was estimated by laboratory-based Ge γ spectrometry. Dose rate calculations were made using DRAC (Durcan et al., 2015). Estimates of radionuclide concentration were converted into D_r values (Guérin et al., 2011), accounting for D_r modulation forced by grain size (Guérin et al., 2012), present moisture content (Zimmerman, 1971; Aitken and Xie, 1990) and, where D_e values were generated from 5-15 μm quartz, reduced signal sensitivity to α radiation (a-value 0.050 ± 0.002). Cosmogenic D_r values were calculated on the basis of sample depth, geographical position and matrix density (Prescott and Hutton, 1994). No samples exhibited pronounced ($^{226}Ra/^{238}U$>50%) U disequilibrium.

S4. Age-Depth Modelling & Accumulation Rate

The determination of the OSL dates allowed detailed age-depth modelling of the alluvial sequence (Figure 2). This was initially conducted using the OSL setting in OxCal, version 4.3 with IntCal[13] program (Bronk Ramsey, 2008; 2009; 2017). Further modelling with Bacon v2.2 (Blaauw and Christen, 2011) enabled a clear improvement in the quality and resolution of the accumulation rate (Fig S1) and enabled the more precise calculation of calendrical dates at 2σ (95.4% confidence) and 1σ (68.2% confidence).

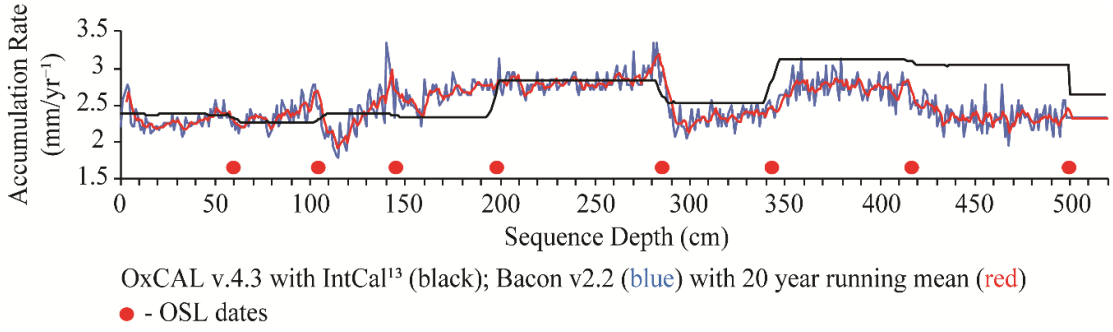

Fig S1. Sediment accumulation rate (mm/yr^{-1}) as modelled by OxCal (black) and Bacon (blue) with 20yr smoothed average (red). Included in Fig.2.

S5. Loss on Ignition (Supplemental Data File 1)

Alongside the chronological determination, samples were also subjected to a range of sedimentological analyses to interpret the depositional history of the sequence. Loss on Ignition (LOI) at 1cm resolution was conducted by combusting samples at 105°C for 12 hours to determine water content, at 550°C for a further 2 hours provided the percentage organics and a final burn at 950°C for 4 hours determined carbonate content (Figure 2).

The clear variation between percentage moisture values between the LOI and OSL method (Supplementary Material S3, Table 1) is a result of differences in sample location. Due to the necessity of getting unaltered dark samples for OSL dating the plastic sample tubes were driven into section and moisture content determined from c.15cm into the section. The LOI samples were determined from the u-channels which were no more than 3cm into the section and therefore demonstrate under representative results. The general trend however of decreasing moisture content up profile is retained in both processes and in most cases the error factors do overlap (Figure S2).

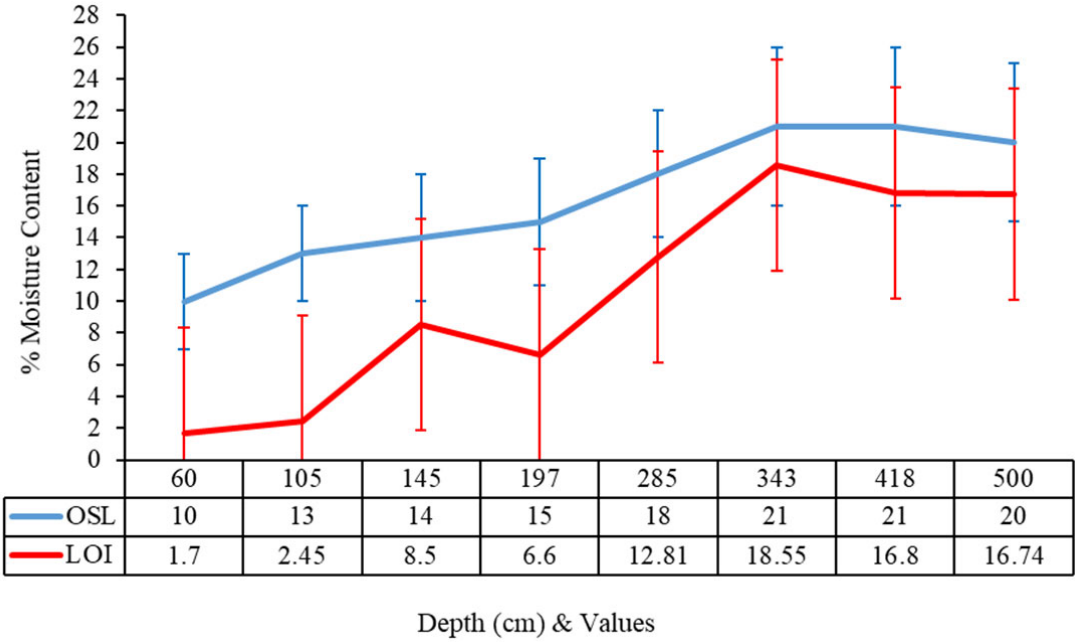

Fig S2. Relative moisture values between OSL and LOI analytical methods.

S6. Magnetic Susceptibility (Supplemental Data File 1)

Magnetic susceptibility (MS) was measured in order to identify high resolution variations in texture, and changes in depositional conditions, as a result of flooding events (Figure 2). The process was also utilised to determine variations in landuse upon the floodplain and has previously shown to demonstrate changes in anthropogenic activity on archaeological sites (Tite and Mullins, 1971). MS was undertaken using a Bartington MS2 meter using the MS2B dual sensor equipment at 1cm resolution. Volume magnetic susceptibility in SI unit (κ) was determined using a fixed frequency of 3.41kHz and a periodicity of 15 seconds, and precision was determined with randomly selected repeatability of samples. The methodology and interpretation of results followed Dearing (1999).

S7. Particle Size Analysis (Supplemental Data File 1)

Further analysis of micro-variant sediment texture was conducted using particle size analysis (Figure 2). Particle size fractions are taken to reflect flow velocities delivered to the floodplain and, as has been shown for the Severn floodplain by Marriott (1992), they will reflect flood velocity if the location of the channel is constant relative to the site. The process was conducted following the methodology set out by Konert and Vandenberghe (1997). 2-5g of sediment was heated to 550^{o}C for 2 hours in a furnace to remove organic material and the remaining sediment sieved through a <2mm sieve and then mixed with a deionized water and Calgon solution to disaggregate remaining components. A subsample of this was then placed into a petrie dish with more Calgon and gently agitated with a pestle before being added to a Malvern Digisizer until an optimal obscuration of 5-20% had been achieved. Background and sample measurement time was set to 90 seconds and each sample was analysed five times in order to get a good statistical dataset as determined by the international standard ISO-13320-1. All samples analysed had a standard deviation lower than 2% for the fine-grained percentile (<Dx10), less than 3% for the median percentile (<Dx50) and less than 5% for the coarsest percentile (<Dx90).

S8. Sediment Power Index (Supplemental Data File 1)

In order to further understand the variations in sediment concentration, size, distribution and presence/absence of void space within the alluvium a Sediment Power Index was calculated (Figure 2). This was achieved by dividing the coarse sediment fraction (Dx90) by the finest sediment fraction (Dx10) to the power 3. The organic fraction was initially removed from the calculation however the LOI at 550 results were so negligible that in the end this was not calculated in the equation.

S9. Multi-element ITRAX analysis (Supplemental Data File 2)

Multi-element determination was calculated using an ITRAX XRF scanner (Croudace et al., 2006). In-situ sediment samples were collected in 400-500mm long 'u channels' from the river section and scanned at 0.2cm resolution using 30kV, 30mA settings and a 15 second count time at the British Ocean Sediment Core Research Facility (BOSCORF) at the National Oceanography Centre, Southampton (NOCS). In total 39 elements were identified including lithogenic indicators (Si, Al, K, Ti, Zr, Rb) and anthropogenic and heavy metal indicators (P, Ca, Cr, Zn, Ba, Sr, Pb). The resultant elemental intensities, measured in total counts per second (tcps), were vetted to remove unreliable results which occurred at the boundaries of samples, in particular within exceptionally coarse sediment horizons. The resultant dataset was then scrutinised and specific combinations of elemental ratios created in order to determine proxy coarse grained indicators (LogZr:Rb) (Jones et al., 2012), flood events (LogZr:Fe) (Wilhelm et al., 2013), redox conditions (LogFe:Mn), and combined heavy metals (Croudace and Rothwell 2015) (Figure 2).

S10. pOSL (Supplemental Data File 3)

Alongside traditional physical and elemental analyses, a programme of portable Optically Stimulated Luminescence (pOSL) analysis was conducted to further detail variations in sediment texture, mineralogical variation, clast content, colour, bleaching (Sanderson and Murphy, 2010). Previous work in fluvial environments (Muñoz-Salinas et al., 2010; Ghilardi et al., 2015; Muñoz-Salinas et al., 2016; Portenga et al., 2016; Gray et al., 2019) has shown that pOSL is also extremely useful in determining sediment provenance, depositional conditions and high-energy flooding events. During the field sampling process, bulk 'dark' samples at 5cm resolution were extracted from 10cm into the cleaned river section, taking care to shield light. The resultant samples were stored in a light proof container and maintained at room temperature. In dark room laboratory conditions, pOSL was measured using the SUERC portable OSL reader and sediment samples stimulated for 60 seconds with the pulsed blue (pOSL) (470nm) and pulsed infrared (pIRSL) (880nm) parts of the electromagnetic spectrum. Data quality was maintained by conducting four sets of independent replicates across sections of the sediment sequence that demonstrated particularly large shifts in results determined in the initial data run. The resultant analysis enabled the determination of Net pIRSL (Figure 2) as well as the Net pOSL and the calculation of pIRSL:pOSL.

S11. Agglomerate Hierarchical Cluster (AHC) (Supplemental Data File 4)

To statistically analyse sedimentological variations within the alluvial sequences from the Severn-Teme confluence at Powick, a programme of Agglomerative Hierarchical Cluster (AHC) analysis was conducted using XLStat 2019.3.2 which enabled the detailed zonation of horizons (Figure 2). Series dissimilarity was determined at 1cm resolution using the Euclidean distance between six variables, percentage organics, percentage carbonate, magnetic susceptibility, fine particulate, percentage sand and LogZr:Rb. Agglomeration was calculated using Ward's Method (Ward, 1963). The results were presented in horizontal dendrograms demonstrating cophenetic distance between variables and horizons, with major classes defined by class colour variation and individual horizon zonation defined by changes at the most similar level (Figure 2).

S12. Principal Component and Variable Factor Analysis (Supplemental Data File 5)

To statistically analyse the comparative nature of actual sediment grain size (ϕ) (Wentworth, 1922) against other grain size proxy indicators (Log carbonate, Log magnetic susceptibility, Log total sand content, Log pIRSL, Log pOSL and LogZr:Rb) Principal Component Analysis and Variable Factor Analysis using Pearson's (n) Correlation was conducted using XLStat 2019.3.2. (Figure 3). Data samples were clustered into 50-year averages to reduce 'noise' and plotted on a combined distance biplot and Varimax rotation plot with an automated coefficient.

S13. Historic and Archaeological Datasets and Flood Records (Figures 1 and 2)

Alongside the quantitative datasets, historic and archaeological information was also added to figures 1 and 2 to assist the overall landuse variation in the confluence landscape. Data sources included the Victoria County History for Worcestershire (Page and Willis-Bund, 1924), place-names (Mawer and Stenton, 1927), archaeological excavation reports (Cook 1996; Edwards and Cook, 2000; Milward, 2005; Vaughan and Wainwright, 2012; Rogers, 2014) and historical texts (Atkin, 1998; 2004).

Data detailing historic floods in the rivers Teme and Middle Severn was gathered from the Chronology of British Hydrological Events (CBHE), University of Dundee (http://cbhe.hydrology.org.uk/) (Black and Law, 2004). Each catchment was investigated, and the number of events tabulated in order to build a frequency per year graph to be interpreted against the other analytical data. Particularly extreme events which covered large areas of the river catchments and where specific historical recording of events occurred in the vicinity of the sample sites were highlighted with an event date on the resultant graphic (Annual Register of the Year 1852, 1853; Marriott and Gaster, 1886; Symons, 1887; Southall, 1895; NERC, 1975; Damari, 1995; Marsh and Dale, 2002; Marsh and Hannaford, 2007). In addition the extent of the major 2007 flood event in the Severn-Teme confluence is depicted using the UK Environment Agency 20cm resolution orthophotography. (UK Environment Agency, 2007) (Figure 2).

S14. Sediment Deposition Models (Supplemental Data File 6)

Sediment Index Models were created for the Severn-Teme confluence at Powick and two other sites, at Broadwas in the Teme and Buildwas in the Severn, to determine wider catchment variation in depositionary processes (Figure 4). These were compiled by normalising coarse and fine sediment grain-size data from Log Grain Size, Carbonate, Magnetic Susceptibility, total sand content, pIRSL, pOSL and LogZr:Rb (Jones et al., 2012). The raw data were statistically tested using polynomial regression and filtered through a 20-year moving average which enabled the identification and refinement of deposition at each site between the Late Iron Age to the present day.

S15. Comparative Climatic Modelling

To compare an extensive range of existing climatic datasets against results gathered from the Severn-Teme confluence at Powick, Comparative Climatic Modelling was conducted on primary data gathered from the Paleoclimatology Data website https://www.ncdc.noaa.gov/data-access/paleoclimatology-data. Relevant data was gathered from six datasets (Charman et al., 2006; Büntgen et al., 2011; Wilson et al., 2013; Phipps et al., 2013; Swindles et al., 2013; Esper et al., 2014) which best demonstrated a range of climatic conditions for the period covered at Powick, and were classed into five geographic regions (UK and Ireland, Northern Europe and Central and Southern Europe) (Figure 4). The raw data was normalised to create 'z-scores' and then graphically illustrated with a 20-year running average to reduce 'noise' and re-interpreted by colour coding to demonstrate relative periods of 'wetter', 'dryer', 'cooler', 'warmer', 'higher solar activity' and 'lower solar activity'.

S16. References

Adamiec, G., and Aitken, M.J., 1998, Dose-rate conversion factors: update: Ancient TL, v. 16, no. 2, p. 37-50, http://ancienttl.org/ATL_16-2_1998/ATL_16-2_Adamiec_p37-50.pdf.

Aitken, M. J., and Xie, J., 1990, Moisture correction for annual gamma dose: Ancient TL, v. 8, no. 2, p. 6-9. http://ancienttl.org/ATL_08-2_1990/ATL_08-2_Aitken_p6-9.pdf

Aitken, M.J., 1998, An introduction to optical dating: the dating of Quaternary sediments by the use of photon-stimulated luminescence: Oxford, Oxford University Press.

Annual Register of the year 1852., 1853, Chronicle section: F. and J. Rivington, London.

Atkin, M., 1998, Cromwell's Crowning Mercy: The Battle of Worcester 1651: Sutton Publishing.

Atkin, M., 2004, Worcestershire Under Arms: An English County During the Civil Wars: Leo Cooper Ltd.

Berger, G.W., Mulhern, P.J., and Huntley, D.J., 1980, Isolation of silt-sized quartz from sediments: Ancient TL, v. 11, p. 8-9, http://ancienttl.org/ATL_L4-2.pdf.

Blaauw, M., and Christen, J.A., 2011, Flexible palaeoclimate age-depth models using an autoregressive gamma process: Bayesian Analysis, v. 6, no. 3, p. 457-474, https://doi.org/10.1214/11-BA618.

Black, A.R. and Law, F.M., 2004, Development and utilization of a national web-based chronology of hydrological events: Hydrological Sciences Journal, v. 49, no. 2, p. 237-246, https://doi.org/10.1623/hysj.49.2.237.34835.

Bøtter-Jensen, L., Mejdahl, V., and Murray, A.S., 1999, New light on OSL: Quaternary Science Reviews, v. 18, no. 2, p. 303-310, https://doi.org/10.1016/S0277-3791(98)00063-8.

British Geological Survey, 2017, Geoindex onshore borehole scans for the Severn-Teme confluence, SO85SW, SO85SE: British Geological Survey, Keyworth, Nottingham, UK, http://mapapps2.bgs.ac.uk/geoindex/home.html.

Bronk Ramsey, C., 2008, Deposition models for chronological records: Quaternary Science Reviews, v. 27, no. 1-2, p. 42-60, https://doi.org/10.1016/j.quascirev.2007.01.019.

Bronk Ramsey, C., 2009, Bayesian analysis of radiocarbon dates: Radiocarbon, v. 51, no. 1, p. 337-360, https://doi.org/10.1017/S0033822200033865.

Bronk Ramsey, C., 2017, Methods for summarizing radiocarbon datasets. Radiocarbon, v. 59, p. 1809-1833, https://doi.org/10.1017/RDC.2017.108.

Brown, A.G., 1983a, Late Quaternary, palaeohydrology, palaeoecology and floodplain development of the lower River Severn, Unpublished PhD thesis, University of Southampton.

Brown, A.G., 1983b, Floodplain deposits and accelerated sedimentation in the lower Severn basin, in: Gregory, K.J., ed., Background to palaeohydrology: Chichester: Wiley, p. 375-397.

Brown, A.G., 1985, Traditional and multivariate techniques in the interpretation of floodplain sediment grain size variations: Earth Surface Processes and Landforms, v. 10, no. 3, p. 281-291, https://doi.org/10.1002/esp.3290100310.

Brown, A.G., 1987, Holocene floodplain sedimentation and channel response of the lower river Severn, U.K.: Zeitscrift fur Geomorphologie N.F., v. 31, p. 293-310.

Büntgen, U., Tegel, W., Nicolussi, K., McCormick, M., Frank, D., Trouet, V., Kaplan, J.O., Herzig, F., Heussner, K-U., Wanner, H., Luterbacher, J., and Esper. J., 2011, 2500 years of European climate variability and human susceptibility: Science, v. 331, no. 6017, p. 578-582, https://doi.org/10.1126/science.1197175 .

Charman, D.J., Blundell, A., Chiverrell, R.C., Hendon, D., and Langdon. P.G., 2006, Compilation of non-annually resolved Holocene proxy climate records: Stacked Holocene peatland palaeo-water table reconstructions from northern Britain: Quaternary Science Reviews, v. 25, no. 3-4, p. 336-350, https://doi.org/10.1016/j.quascirev.2005.05.005

Chronology of British Hydrological Website (http://cbhe.hydrology.org.uk/): University of Dundee & British Hydrological Society [Accessed April 2019].

Cook, M., 1996, Archaeological recording at Powick Weir, near Worcester: Report 505, project 1309, Historic Environment and Archaeology Service, Worcestershire County Council, Worcester, https://public.worcestershire.gov.uk/sites/archaeology/Reports/wr4815.pdf.

Coventry Map, c.1648, Herefordshire and Worcestershire Record Office, BA940, folio 970.7.73.

Croudace, I., and Rothwell, R.G., eds, 2015, Micro-XRF studies of sediment cores: applications of a non-destructive tool for the environmental sciences: London, Springer.

Croudace, I.W., Rindby, A., and Rothwell, R.G., 2006, ITRAX: description and evaluation of a new multi-function X-ray core scanner: Geological Society Special Publications, v. 267, no. 1, p. 51-63, https://doi.org/10.1144/GSL.SP.2006.267.01.04.

Damari, P., 1995, The Herefordshire and Worcestershire weather book: Countryside Books, Newbury, Berkshire.

Dearing, J., 1999, Magnetic susceptibility, *in* Walden, J., Smith, J.P., and Oldfield, F., eds, Environmental magnetism, a practical guide: Quaternary Research Association. Technical Guide no. 6, p. 35-62.

Duller, G.A.T., 2003, Distinguishing quartz and feldspar in single grain luminescence measurements: Radiation Measurements, v. 37, no. 2, p. 161-165, https://doi.org/10.1016/S1350-4487(02)00170-1.

Duller, G.A.T. 2015, The Analyst software package for luminescence data: overview and recent improvements: Ancient TL, v. 33, no.1, p. 35-42, http://ancienttl.org/ATL_33-1_2015/ATL_33-1_Duller_p35-42.pdf.

Durcan, J.A., King, G.E. and Duller, G.A.T. 2015, DRAC: Dose rate and age calculator for trapped charge dating: Quaternary Geochronology, v. 28, p. 54-61, https://doi.org/10.1016/j.quageo.2015.03.012.

Edwards, R. and Cook, M., 2000, Watching brief at Powick Weir, Powick and Lower Wick, Worcestershire: Report 1635, Historic Environment and Archaeology Service, Worcestershire County Council, Worcester, https://public.worcestershire.gov.uk/sites/archaeology/Reports/wr6422.pdf.

Esper, J., Düthorn, E., Krusic, P.J., Timonen, M., and Büntgen, U., 2014, Northern European summer temperature variations over the Common Era from integrated tree-ring density records: Journal of Quaternary Science, v. 29, no. 5, p. 487-494, https://doi.org/10.1002/jqs.2726.

Ghilardi, M., Sanderson, D., Kinnaird, T., Bickett, A., Balossino, S., Parisot, J-C., Hermitte, D., Guibal, F., and Fleury, J.T., 2015, Dating the bridge at Avignon (south France) and reconstructing the Rhone River fluvial palaeo-landscape in Provence from medieval to modern times: Journal of Archaeological Science: v. 4, p. 336-354, https://doi.org/10.1016/j.jasrep.2015.10.002.

Gray, H.J., Jain, M., Sawakuchi, A.O., Mahan, S.A., and Tucker, G.E., 2019, Luminescence as a sediment tracer and provenance tool: Reviews of Geophysics, v. 57, no. 3, p. 987-1017, https://doi.org/10.1029/2019RG000646.

Guérin, G., Mercier, N., and Adamiec, G. 2011, Dose-rate conversion factors: update: Ancient TL, v. 29, no. 1, p. 5-8, http://ancienttl.org/ATL_29-1_2011/ATL_29-1_Guerin_p5-8.pdf.

Guérin, G., Mercier, N., Nathan, R., Adamiec, G., and Lefrais, Y., 2012, On the use of the infinite matrix assumption and associated concepts: a critical review: Radiation Measurements, v. 47, no. 9, p. 778-785, https://doi.org/10.1016/j.radmeas.2012.04.004.

Huntley, D.J., Godfrey-Smith, D.I., and Thewalt, M.L.W, 1985, Optical dating of sediments: Nature, v. 313, p. 105-107. https://doi.org/10.1038/313105a0

Hütt, G., Jaek, I., and Tchonka, J., 1988, Optical dating: K-feldspars optical response stimulation spectra: Quaternary Science Reviews, v. 7, no. 3-4, p. 381-385, https://doi.org/10.1016/0277-3791(88)90033-9.

Jackson, M.L., Sayin, M., and Clayton, R.N., 1976, Hexafluorosilicic acid reagent modification for quartz isolation: Soil Science Society of America Journal, v. 40, no. 6, p. 958-960, https://doi.org/10.2136/sssaj1976.03615995004000060040x.

Jones, A.F., Macklin, M.G., and Brewer, P.A., 2012, A geochemical record of flooding on the upper river Severn, UK, during the last 3750 years: Geomorphology, v. 179, p. 89-105, https://doi.org/10.1016/j.geomorph.2012.08.003.

Konert, M. and Vandenberghe, J.E.F., 1997, Comparison of laser grain size analysis with pipette and sieve analysis: A solution for the underestimation of the clay fraction: Sedimentology, v. 44, no. 3, p. 523-535, http://dx.doi.org/10.1046/j.1365-3091.1997.d01-38.x.

Markey, B.G., Bøtter-Jensen, L., and Duller, G.A.T., 1997, A new flexible system for measuring thermally and optically stimulated luminescence: Radiation Measurements, v. 27, no. 2, p. 83-89, https://doi.org/10.1016/S1350-4487(96)00126-6.

Marriott, S., 1992, Textual analysis and modelling of a flood deposit: River Severn, U.K.: Earth Surface Processes and Landforms, v. 17, no. 7, p. 687-697, https://doi.org/10.1002/esp.3290170705.

Marriott, W. and Gaster, F., 1886, The Floods of May 1886: Quarterly Journal of the Royal Meteorological Society, v. XII, p 280-282.

Marsh, T.J. and Hannaford, J., 2007, The summer 2007 floods in England and Wales – a hydrological appraisal: Centre for Ecology and Hydrology. Centre for Ecology & Hydrology, Wallingford.

Marsh, T.J., and Dale, M., 2002, The UK floods of 2000-2001: A hydrometeorological appraisal: Water and Environment Journal, v. 16, no. 3, p. 180 – 188, https://doi.org/10.1111/j.1747-6593.2002.tb00392.x.

Mawer, A. and Stenton, F.W., 1927, The place names of Worcestershire: English Place-Name Society, Cambridge, v. 4.

Mejdahl, V., 1979, Thermoluminescence dating: beta-dose attenuation in quartz grains: Archaeometry, v. 21, no. 1, p. 61-72, https://doi.org/10.1111/j.1475-4754.1979.tb00241.x.

Milward, J. 2005, Archaeological evaluation at Manor Farm, Powick, Worcestershire: Report 1374, project 2774, Historic Environment and Archaeology Service, Worcestershire County Council, Worcester, https://public.worcestershire.gov.uk/sites/archaeology/Reports/wr5270.pdf.

Muñoz-Salinas, E., Bishop, P., Sanderson, D.C.W., and Zamorano, J-J., 2010, Interpreting luminescence data from a portable OSL reader: three case studies in fluvial settings: Earth Surface Processes and Landforms, v. 36, no. 5, p.651-660, https://doi.org/10.1002/esp.2084.

Muñoz□Salinas, E., Castillo, M., Sanderson, D., Kinnaird, T., and Cruz□Zaragoza, E., 2016, Using three different approaches of OSL for the study of young fluvial sediments at the coastal plain of the Usumacinta–Grijalva River Basin, southern Mexico: Earth Surface Processes and Landforms, v. 41, no. 6, p. 823–834, https://doi.org/10.1002/esp.3880.

Murray, A.S., and Wintle, A.G., 2000, Luminescence dating of quartz using an improved single-aliquot regenerative-dose protocol: Radiation Measurements, v. 32, no. 1, p. 57-73, https://doi.org/10.1016/S1350-4487(99)00253-X.

Murray, A.S., and Wintle, A.G., 2003, The single aliquot regenerative dose protocol: potential for improvements in reliability: Radiation Measurements, v. 37, no. 4-5, p. 377-381, https://doi.org/10.1016/S1350-4487(03)00053-2.

NERC, 1975, Flood Studies Report. vol 4: Meteorological Studies, Natural Environment Research Council, Swindon, UK.

Page, W. and Willis-Bund, J.W., (eds), 1924, Victoria History of the County of Worcestershire, IV.

Phipps, S.J., McGregor, H.V., Gergis, J., Gallant, A.J.E., Neukom, R., Stevenson, S., Ackerley, D., Brown, J.R., Fischer, M.J., and van Ommen, T.D., 2013, Paleoclimate data-model comparison and the role of climate forcings over the past 1500 years: Journal of Climate, v. 26, no. 18, p. 6915-6936, https://doi.org/10.1175/JCLI-D-12-00108.1.

Portenga, E.W., Bishop, P., Gore, D.B., and Westaway, K.E., 2016, Landscape preservation under post□European settlement alluvium in the south□eastern Australian tablelands, inferred from portable OSL reader data: Earth Surface Processes and Landforms, v. 41, no. 12, p. 1697–1707, https://doi.org/10.1002/esp.3942.

Prescott, J.R., and Hutton, J.T., 1994, Cosmic ray contributions to dose rates for luminescence and ESR dating: large depths and long-term time variations: Radiation Measurements, v. 23, no. 2-3, p. 497-500, https://doi.org/10.1016/1350-4487(94)90086-8.

Rogers, T., 2014, Excavation at Bath Road, Worcester, 2006: Worcestershire Archaeology Research Report No. 1, Worcestershire County Council, Worcester.

Sanderson, D.C.W. and Murphy, S., 2010, Using simple portable OSL measurements and laboratory characterisation to help understand complex and heterogeneous sediment sequences for

luminescence dating: Quaternary Geochronology, v. 5, no. 2-3, p. 299-305, https://doi.org/10.1016/j.quageo.2009.02.001

Southall, H., 1895, Floods in the West Midlands: Quarterly Journal Royal Meteorological Society v. XXI, p.88.

Swindles, G.T., Lawson, I.T., Matthews, I.P., Blaauw, M., Daley, T.J., Charman, D.J., Roland, T.P., Plunkett, G., Schettler, G., Gearey, B.R., Turner, T.E., Rea, H.A., Roe, H.M., Amesbury, M.J., Chambers, F.M., Holmes, J., Mitchell, F.J.G., Blackford, J., Blundell, A., Branch, N., Holmes, J., Langdon, P., McCarroll, J., McDermott, F., Oksanen, P.O., Pritchard, O., Stastney, P., Stefanini, B., Young, D., Wheeler, J., Becker, K. and Armit, I., 2013, Centennial-scale climate change in Ireland during the Holocene: Earth-Science Reviews, v. 126, p. 300-320, https://doi.org/10.1016/j.earscirev.2013.08.012.

Symons, G.J., 1887, British Rainfall for 1886. On the distribution of rain over the British Isles during the year 1886 as observed at nearly 2500 stations in Great Britain and Ireland: G. Shield, London, www.metoffice.gov.uk/learning/library/archive-hidden-treasures/british-rainfall.

Tite, M.S., and Mullins, C., 1971, Enhancement of the magnetic susceptibility of soils on archaeological sites: Archaeometry, v. 13, no. 2, p. 209-219, https://doi.org/10.1111/j.1475-4754.1971.tb00043.x.

Toms, P.S., and Wood, J.C., 2018, Optical dating of sediments: Powick, UK: Unpublished technical report from the Luminescence Dating Laboratory, University of Gloucestershire.

Vaughan, T.M. and Wainwright, J., 2012, Archaeological evaluation of Plot 32, South Worcester, Worcester Road, Broomhall, Worcestershire: Report No. 1924, Worcestershire Archaeology, Worcestershire County Council, https://public.worcestershire.gov.uk/sites/archaeology/Reports/SWR22555.pdf.

UK Environment Agency, 2007, 20cm resolution orthophotography of the Severn-Teme confluence during 2007 flood for grid squares SO85SW, SO85SE. Department for Environment, Food and Rural Affairs, HMSO. Extracted and downloaded [20-07-2017]. https://environment.data.gov.uk/DefraDataDownload/?Mode=survey.

UK Environment Agency, 2016, Raw lidar data, 1m DTM (2016) for SO85SW, SO85SE: Department for Environment, Food and Rural Affairs, HMSO. Extracted and downloaded [20-07-2017] https://environment.data.gov.uk/DefraDataDownload/?Mode=survey.

UK Ordnance Survey County Series 1st Edition, 1886, [TIFF geospatial data], scale 1:2500, Tiles: worc-so8149-1,worc-so8150-1,worc-so8151-1,worc-so8152-1,worc-so8249-1,worc-so8250-1,worc-so8251-1,worc-so8252-1,worc-so8349-1,worc-so8350-1,worc-so8351-1,worc-so8352-1,worc-so8449-1,worc-so8450-1,worc-so8451-1,worc-so8452-1, Updated: 30 November 2010, Historic. Extracted and downloaded from Edina Historic Digimap Service [20-07-2017]. http://digimap.edina.ac.uk.

UK Ordnance Survey, 2016, Raw lidar data, 50m DTM for grid squares SO85SW, SO85SE 1:50,000: Ordnance Survey Open Data Licence, Crown copyright. Extracted and downloaded from Edina digimap [20-07-2017] https://digimap.edina.ac.uk/roam/download/os.

Ward, J. H., Jr., 1963, Hierarchical grouping to optimize an objective function: Journal of the American Statistical Association, v. 58, no. 30, p. 236-244, http://www.jstor.org/stable/2282967?origin=JSTOR-pdf.

Wentworth, C. K, 1922. A scale of grade and class terms for clastic sediments: The Journal of Geology, v. 30, no. 5, p. 377–392, https://www.jstor.org/stable/30063207.

WHER, 2017, Worcestershire Historic Environment Record online database http://www.worcestershire.gov.uk/archaeology. [accessed 2017].

Wilhelm B., Arnaud, F., Sabatier, P., Magand, O., Chapron, E., Courp, T., Tachikawa, K., Fanget, B., Malet, E., Pignol, C., Bard, E., Delannoy, J.J., 2013, Palaeoflood activity and climate change over the last 1400 years recorded by lake sediments in the north-west European Alps: Journal of Quaternary Science, v. 28, no. 2, p. 189-199, https://doi.org/10.1002/jqs.2609

Wilson, R.J.S., Miles, D.W.H., Loader, N.J., Melvin, T.M., Cunningham, L.K., Cooper, R.J., and Briffa, K.R., 2013, A millennial long March-July precipitation reconstruction for southern-central England: Climate Dynamics, v. 40, no. 3-4, p. 997-1017, https://doi.org/10.1007/s00382-012-1318-z.

Zimmerman, D.W., 1971, Thermoluminescent dating using fine grains from pottery: Archaeometry, v. 13, no. 1, p. 29-52, https://doi.org/10.1111/j.1475-4754.1971.tb00028.x.

Lab Code	Overburden (m)	Grain size (μm)	Moisture content (%)	NaI γ-spectrometry (*in situ*) γ D_r ($Gy.ka^{-1}$)	Ge γ-spectrometry (*ex situ*)			α D_r ($Gy.ka^{-1}$)	β D_r ($Gy.ka^{-1}$)	Cosmic D_r ($Gy.ka^{-1}$)	$^{226}Ra/^{238}U$	Total Dr ($Gy.ka^{-1}$)	Preheat (°C for 10s)	Low Dose Recycling Ratio	High Dose Recycling Ratio	Post-IR OSL Ratio	D_e (Gy)	Age (ka)	cal. BCE/CE date (σ2 95.4%)	cal. BCE/CE date (σ1 68.2%)
					K (%)	Th (ppm)	U (ppm)													
GL17016	0.60	125-180	10 ± 3	0.86 ± 0.04	1.20 ± 0.09	9.76 ± 0.59	1.72 ± 0.14	-	1.17 ± 0.08	0.19 ± 0.02	0.88 ± 0.14	2.22 ± 0.09	280	0.97 ± 0.05	0.99 ± 0.03	0.95 ± 0.04	0.5 ± 0.1	0.25 ± 0.04	cal.CE1691-1849	cal.CE1731-1810
GL17015	1.05	5-15	13 ± 3	0.97 ± 0.05	1.61 ± 0.10	10.32 ± 0.60	1.98 ± 0.14	0.50 ± 0.04	1.59 ± 0.09	0.18 ± 0.02	0.78 ± 0.10	3.23 ± 0.11	260	0.92 ± 0.17	0.98 ± 0.10	0.91 ± 0.17	1.5 ± 0.1	0.46 ± 0.03	cal.CE1503-1585	cal.CE1530-1585
GL17014	1.45	5-15	14 ± 4	0.96 ± 0.05	1.71 ± 0.11	9.97 ± 0.59	1.87 ± 0.14	0.47 ± 0.04	1.61 ± 0.14	0.16 ± 0.02	0.86 ± 0.11	3.20 ± 0.13	260	1.00 ± 0.16	0.99 ± 0.09	1.04 ± 0.17	2.0 ± 0.1	0.63 ± 0.04	cal.CE1314-1464	cal.CE1352-1426
GL17013	1.97	5-15	15 ± 4	0.95 ± 0.05	1.58 ± 0.10	10.40 ± 0.60	1.93 ± 0.14	0.48 ± 0.04	1.53 ± 0.10	0.15 ± 0.01	1.03 ± 0.13	3.10 ± 0.12	260	1.01 ± 0.15	1.02 ± 0.08	0.99 ± 0.15	2.8 ± 0.1	0.91 ± 0.06	cal.CE995-1217	cal.CE1051-1161
GL17012	2.85	5-15	18 ± 4	1.01 ± 0.05	1.80 ± 0.11	10.99 ± 0.64	2.15 ± 0.15	0.50 ± 0.04	1.66 ± 0.10	0.13 ± 0.01	0.81 ± 0.09	3.30 ± 0.12	240	0.99 ± 0.10	0.97 ± 0.06	1.01 ± 0.10	3.7 ± 0.1	1.13 ± 0.06	cal.CE763-1010	cal.CE825-948
GL17011	3.43	5-15	21 ± 5	0.97 ± 0.06	1.83 ± 0.11	10.91 ± 0.63	2.01 ± 0.14	0.47 ± 0.04	1.61 ± 0.11	0.12 ± 0.01	1.04 ± 0.12	3.17 ± 0.13	240	0.98 ± 0.10	0.99 ± 0.07	0.97 ± 0.10	4.8 ± 0.2	1.52 ± 0.09	cal.CE323-678	cal.CE412-590
GL17010	4.18	5-15	21 ± 5	0.99 ± 0.06	1.82 ± 0.11	10.71 ± 0.63	2.31 ± 0.15	0.49 ± 0.04	1.64 ± 0.11	0.11 ± 0.01	0.98 ± 0.12	3.22 ± 0.13	240	0.99 ± 0.10	1.02 ± 0.08	1.02 ± 0.11	5.1 ± 0.2	1.59 ± 0.09	cal.CE244-615	cal.CE337-552
GL17009	5.00	5-15	20 ± 5	1.00 ± 0.06	1.85 ± 0.11	10.99 ± 0.63	2.15 ± 0.15	0.49 ± 0.04	1.66 ± 0.11	0.09 ± 0.01	0.97 ± 0.12	3.24 ± 0.13	260	0.95 ± 0.08	1.00 ± 0.07	0.99 ± 0.08	5.6 ± 0.2	1.74 ± 0.10	cal.CE68-482	cal.CE172-379

Table S1. D_r, D_e and Age data of submitted samples from THE Severn-Teme confluence at Powick, Worcestershire (Lat: 52.169259, Lon:-2.2376946). Age estimates expressed relative to 2017. Uncertainties in age are quoted at 2σ (95.4%) and 1σ (68.2%) confidence and reflect combined systematic and experimental variability.